



## Global Biogeochemical Cycles

### RESEARCH ARTICLE

10.1002/2017GB005624

#### Key Points:

- Perfluorooctane sulfonate (PFOS) shows promise as a new ocean tracer but is also a potent toxicant
- PFOS concentrations in the upper North Atlantic Ocean peaked between 2002 and 2005 but are still increasing in the deep ocean.
- Sinking, convection, and southward transport of subpolar surface waters greatly reduces PFOS inputs to the high Arctic

#### Supporting Information:

- Supporting Information S1

#### Correspondence to:

X. Zhang,  
xianmingzhang@g.harvard.edu

#### Citation:

Zhang, X., Y. Zhang, C. Dassuncao, R. Lohmann, and E. M. Sunderland (2017), North Atlantic Deep Water formation inhibits high Arctic contamination by continental perfluorooctane sulfonate discharges, *Global Biogeochem. Cycles*, 31, doi:10.1002/2017GB005624.

Received 17 JAN 2017

Accepted 31 JUL 2017

Accepted article online 4 AUG 2017

## North Atlantic Deep Water formation inhibits high Arctic contamination by continental perfluorooctane sulfonate discharges

Xianming Zhang<sup>1,2</sup> , Yanxu Zhang<sup>1</sup>, Clifton Dassuncao<sup>1,2</sup> , Rainer Lohmann<sup>3</sup>, and Elsie M. Sunderland<sup>1,2</sup> 

<sup>1</sup>Harvard John A. Paulson School of Engineering and Applied Sciences, Harvard University, Cambridge, Massachusetts, USA,

<sup>2</sup>Department of Environmental Health, Harvard T. H. Chan School of Public Health, Boston, Massachusetts, USA, <sup>3</sup>Graduate School of Oceanography, University of Rhode Island, Narragansett, Rhode Island, USA

**Abstract** Perfluorooctane sulfonate (PFOS) is an aliphatic fluorinated compound with eight carbon atoms that is extremely persistent in the environment and can adversely affect human and ecological health. The stability, low reactivity, and high water solubility of PFOS combined with the North American phaseout in production around the year 2000 make it a potentially useful new tracer for ocean circulation. Here we characterize processes affecting the lifetime and accumulation of PFOS in the North Atlantic Ocean and transport to sensitive Arctic regions by developing a 3-D simulation within the MITgcm. The model captures variability in measurements across biogeographical provinces ( $R^2 = 0.90$ ,  $p = 0.01$ ). In 2015, the North Atlantic PFOS reservoir was equivalent to 60% of cumulative inputs from the North American and European continents (1400 Mg). Cumulative inputs to the Arctic accounted for 30% of continental discharges, while the remaining 10% was transported to the tropical Atlantic and other regions. PFOS concentrations declined rapidly after 2002 in the surface mixed layer (half-life: 1–2 years) but are still increasing below 1000 m depth. During peak production years (1980–2000), plumes of PFOS-enriched seawater were transported to the sub-Arctic in energetic surface ocean currents. However, Atlantic Meridional Overturning Circulation (AMOC) and deep ocean transport returned a substantial fraction of this northward transport (20%, 530 Mg) to southern latitudes and reduced cumulative inputs to the Arctic (730 Mg) by 70%. Weakened AMOC due to climate change is thus likely to increase the magnitude of persistent bioaccumulative pollutants entering the Arctic Ocean.

**Plain Language Summary** Perfluorooctane sulfonate (PFOS) is a persistent anthropogenic compound that has been released to the environment in large quantities and adversely affects human and ecological health. Its production was phased out in North America in 2000, but the ocean is the terminal PFOS sink. This study develops a new model for PFOS cycling in the North Atlantic Ocean and transport to sensitive Arctic regions based on best understanding of ocean physics and ecology. Results suggest that in 2015, 60% of cumulative PFOS discharges from North America and Europe were still present in the North Atlantic and 30% had entered the Arctic Ocean. Most of the remaining fraction was transported to the South Atlantic. The lifetime of PFOS in the surface ocean is less than 5 years due to rapid penetration into deeper waters where it persists for decades or longer before being transported to other basins. During peak production years, most continental PFOS pollution was transported to the sub-Arctic but large-scale overturning of the North Atlantic Ocean reduced the total burden entering the high Arctic by 70%. Climate-driven changes in ocean circulation that are weakening this process may thus increase the vulnerability of the Arctic to continental pollution.

### 1. Introduction

Perfluorooctane sulfonate (PFOS) is an aliphatic organofluorine molecule containing eight carbon atoms, a highly fluorinated “tail,” and a hydrophilic sulfonate “head” group. It has been transported in wastewater and rivers to the global oceans as a terminal sink after use in furniture and carpet coatings, food packaging, nonstick cookware, outdoor clothing/gear, and industrial applications since the 1950s [Wang et al., 2017]. Biomonitoring studies have revealed high PFOS concentrations in many marine food webs and exposures pose risks to both human and ecological health [Tomy et al., 2004; Dassuncao et al., 2017]. PFOS does not appreciably degrade under environmental conditions due to the strength of carbon-fluorine bonds [Wang

*et al.*, 2015]. It is not volatile and has much higher water solubility and lower affinity for partitioning to particles than other hydrophobic organic pollutants such as polychlorinated biphenyls (PCBs) [Muir and Lohmann, 2013; Zareitalabad *et al.*, 2013; Rayne and Forest, 2009]. Thus, Yamashita *et al.* [2008] proposed it as a novel tracer for ocean circulation. However, little is known about the distribution and accumulation of PFOS in the global oceans. Here we investigate processes driving the lifetime and accumulation of PFOS in the North Atlantic Ocean and its transport to vulnerable Arctic regions by developing a new simulation within a 3-D ocean circulation model (MITgcm).

Globally, chemical manufacturing by the 3M Company in Decatur, Alabama, USA, accounted for most (~80%) of the 66,000 t of PFOS produced between 1958 and 2000 [Armitage *et al.*, 2009a]. 3M voluntarily discontinued manufacturing of the PFOS parent chemical between 2000 and 2002, amid concerns about human and ecological health impacts [Land *et al.*, 2015]. Some PFOS has been produced in Asia after 2000, but most chemical manufacturing has shifted to other fluorinated compounds with different carbon chain lengths and head groups in the larger family of polyfluoroalkyl and perfluoroalkyl substances (PFASs) [Wang *et al.*, 2017]. The phaseout in North American PFOS production adds to its potential utility as a tracer for ocean water mass ages and circulation.

On the continental scale, wastewater is thought to account for the majority of PFOS releases (~85%) to the environment [Buser and Morf, 2009; Earnshaw *et al.*, 2014]. Atmospheric emissions of unstable PFOS precursors can also occur during chemical manufacturing but are estimated to account for only 1% of total inputs to the ocean [Armitage *et al.*, 2009a]. The impact of changes in PFOS production on continental discharges and subsequent accumulation in the ocean is poorly understood. Prior work suggests vertical diffusion and sorption to settling particles are important for oceanic transport of PFASs [Lohmann *et al.*, 2013; Sanchez-Vidal *et al.*, 2015]. Seawater PFOS measurements are limited and modeling studies have not previously resolved basin-scale inputs and circulation [Armitage *et al.*, 2009a; Schenker *et al.*, 2008]. The only prior ocean model for PFOS contained 18° latitudinal bands for the globe and did not distinguish the Atlantic and Pacific basins [Armitage *et al.*, 2009a]. Previous modeling studies for other PFASs similarly do not consider spatial variability in oceanic concentrations and transport or lack detailed release estimates for continental discharges [Armitage *et al.*, 2009b; Wania, 2007; Stemmler and Lamme, 2010].

The main objectives of this work are to (1) quantify the magnitude and spatial distribution of continental PFOS discharges to the North Atlantic Ocean and (2) better characterize the roles of lateral and vertical transport processes for the distribution and lifetime of PFOS in the marine water column. We develop an inventory of cumulative continental PFOS releases from wastewater and rivers in North America and Europe between 1958 and 2010 and use it to force a new 3-D simulation for the North Atlantic Ocean within the MITgcm [Marshall *et al.*, 1997]. We evaluate the model using available seawater PFOS measurements and apply it to investigate how changing releases have affected spatial and temporal variability in concentrations and inputs to the Arctic Ocean. This information is needed to further assess the potential viability of PFOS as a tracer for oceanic transport processes as well as its significance as a toxicant in marine food webs since biological exposures are driven by seawater concentrations.

## 2. Model Description

The MITgcm is an ocean general circulation model (<http://mitgcm.org>) that contains a biogeochemical and ecological model for cycling of carbon, nitrogen, silica, phosphorus, and iron through inorganic, living plankton (phytoplankton and zooplankton), and dead organic matter [Dutkiewicz *et al.*, 2009]. It has a horizontal resolution of  $1^\circ \times 1^\circ$  and includes 23 vertical levels. Ocean state estimates are based on the Estimating Circulation and Climate of the Ocean (ECCO-GODAE) data product [Marshall *et al.*, 1997; Wunsch and Heimbach, 2007]. We added tracers for the dissolved and particle-bound forms of PFOS that are transported laterally and vertically by oceanic circulation, mixing and particle settling.

PFOS has a  $pK_a$  of negative three and is extremely stable in solution [Campbell *et al.*, 2009; Cheng *et al.*, 2009; Vecitis *et al.*, 2008]. Partitioning between the aqueous phase and suspended particles is simulated using an empirically derived organic carbon normalized partition coefficient ( $\log K_{oc} = 2.6$ ) [Higgins and Luthy, 2006]. Particle concentrations, composition, and export fluxes are based on the ecology simulation embedded in the MITgcm [Dutkiewicz *et al.*, 2009] and used to simulate vertical PFOS transport associated with settling particles.

The model is initialized by assuming zero oceanic PFOS concentrations before 1958, the onset of chemical production. For the years 1958 to 2010, the model is forced with  $1^\circ \times 1^\circ$  gridded inputs to the North Atlantic Ocean between  $20^\circ\text{N}$  and  $60^\circ\text{N}$  from rivers and wastewater treatment plants in North America and Europe using the inventory developed here. The simulation is continued with zero inputs between 2010 and 2038 to capture the phaseout in PFOS production. We divide annual inputs equally over each 3 h time step in the model simulation because available monitoring data do not show significant seasonal differences (supporting information Table S1) [Boulanger *et al.*, 2004; Schultz *et al.*, 2006; Loganathan *et al.*, 2007; Plumlee *et al.*, 2008; Erickson *et al.*, 2009; Furl *et al.*, 2011; Furdui *et al.*, 2008; D'eon *et al.*, 2009; Guerra *et al.*, 2014].

### 3. Continental PFOS Release Inventory (1958–2010)

We developed a time-dependent inventory of PFOS inputs from wastewater treatment plants and rivers to the North Atlantic between 1958 and 2010. We neglect PFOS originating from degradation of atmospheric precursors because atmospheric inputs to the ocean are thought to be small [Armitage *et al.*, 2009a].

PFOS inputs from European rivers to the North Atlantic (Figure S1) are based on monitoring data for 2006–2007 and the relationship derived by Pistocchi and Loos [2009] between measured PFOS concentrations in river water ( $E_R$ ,  $\text{kg a}^{-1}$ ) and population within a watershed basin ( $P_B$ ):

$$E_R = 9.6 \times 10^{-9} P_B^{1.0115} \quad (1)$$

To estimate temporal changes in loading, we scaled per-capita releases calculated from gridded European population data [Center for International Earth Science Information Network, Columbia University *et al.*, 2005] by relative changes in annual production of the parent chemical to PFOS (perfluorooctane sulfonyl fluoride: POSF) for all years between 1958 and 2010 [Armitage *et al.*, 2009a; Paul *et al.*, 2009; Zhang *et al.*, 2012].

Comprehensive riverine PFOS monitoring data are not available for North America for any year. Thus, we compiled PFOS wastewater monitoring data (Table S1 and Figure S2) from 19 Canadian facilities between 2009 and 2010 [Guerra *et al.*, 2014] and 36 U.S. facilities in 2007 [Erickson *et al.*, 2009]. Following Pistocchi and Loos [2009], we related PFOS releases ( $E_W$ ,  $\mu\text{g d}^{-1}$ ) to population served ( $P_W$ ) using power regression analysis:

$$E_W = \beta P_W^\alpha \quad (2)$$

where  $\beta$  represents the baseline per-capita PFOS discharge rate, which is equal to 0.21 for Canada and 0.47 for the U.S. (Figure S3). The parameter  $\alpha$  is a scaling factor representing a nonlinear increase in PFOS releases with population served, equal to  $1.24 \pm 0.09$  for Canada and  $1.21 \pm 0.10$  for the U.S. (Figure S3).

Only 9.9% of the municipalities in Canada [Environment Canada, 2009] and 1.8% of wastewater treatment plants in the U.S. [U.S. Environmental Protection Agency (EPA), 2008] discharge directly into the North Atlantic (Figure S4 and Table S2). To calculate wastewater PFOS inputs to river basins that enter the North Atlantic Ocean (Figure S5 and Table S3), we summed PFOS discharges derived from the total populations served by wastewater treatment facilities within each catchment using ArcGIS [Environment Canada, 2009; Global Runoff Data Centre, 2007; U.S. EPA, 2008]. We also included direct releases (360 Mg during 1958–2002) from the 3M Decatur (Alabama) facility to the Mississippi watershed that accounted for a large fraction of global production in 2002 [Armitage *et al.*, 2009a; Filipovic *et al.*, 2013; Scott *et al.*, 2009; 3M, 2000]. We neglected other environmental release pathways such as leaching from landfills because they comprise <10% of total releases on the continental scale, even though they can be important for inland rivers and streams [e.g., Zhang *et al.*, 2016]. We derived basin wide releases ( $\mu\text{g person}^{-1} \text{a}^{-1}$ ) based on wastewater treatment plants within each catchment area [CIESN, 2005]. Temporal changes in global historical inventories [Armitage *et al.*, 2009b; Wang *et al.*, 2014a] were used to scale population-based releases over the full history of production.

There are no data available for riverine or wastewater PFOS discharges in North Africa, Mexico, and Central America. We assumed that population-based PFOS emission factors were approximately 1 order of magnitude lower than those in Northern Europe based on wastewater monitoring data (Figure S6) from other

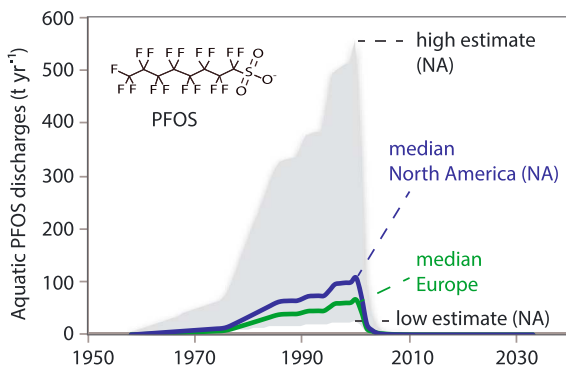


**Figure 1.** Direct continental inputs of PFOS to the North Atlantic Ocean ( $20^{\circ}$  N– $60^{\circ}$  N) from European and North American (U.S. and Canada) wastewater and rivers between 1958 and 2010. Median estimates are shown as the solid line and shaded grey indicates 95% confidence intervals for North American releases. European inputs are based on *Pistocchi and Loos* [2009].

lag time in a one-box model to measured PFOS concentrations leaving these systems, given inputs estimated from this work (Table S4). Resulting lag times ranged between 1.5 and 2.5 years. We did not use the residence time for each of these water bodies because we do not expect PFOS to be well mixed.

### 3.1. Uncertainty in Release Estimates

We estimate a five-fold uncertainty in continental PFOS discharges presented here based on the 95% confidence intervals of regression relationships for the U.S. and Canada (Figure S3). We propagate this uncertainty for evaluation of model results and use available measurements to constrain inputs. Uncertainty estimated here is slightly lower than the approximately 1 order of magnitude uncertainty for other PFAS inventories. In prior work, uncertainty estimates reflected limited information on the magnitude of PFASs emissions from products containing these compounds, assumptions about yields of atmospheric precursors, and ranges in industrial release estimates [Prevedouros et al., 2006; Paul et al., 2009; Armitage et al., 2009a, 2009b; Wang et al., 2014a, 2014b].

### 4. Model Evaluation

The median discharge scenario based on wastewater and riverine monitoring data suggests that  $2.7 \times 10^3$  Mg PFOS has cumulatively entered the North Atlantic since 1958 (low bound:  $5.3 \times 10^2$  Mg, high bound  $1.3 \times 10^4$  Mg, Figure 1). North American coastal releases accounted for 59% of total releases, and the remaining 41% was from Europe (Figure 1). Inputs to the North Atlantic peaked in the year 2000 and declined to negligible amounts by 2010 (Figure 1). For the median release scenario, an additional  $1.5 \times 10^3$  Mg of PFOS flowed into the North Atlantic indirectly from the Gulf of Mexico and Mediterranean Sea.

Direct release values from two previous PFOS inventories based on chemical production and product use are comparable to the low and median bounds for this work. Armitage et al. [2009a] suggested cumulative direct global releases to the ocean of  $2.8 \times 10^2$  to  $2.3 \times 10^3$  Mg between the years 1957 and 2002. Most releases were concentrated in North America and Europe between  $36$  and  $54^{\circ}$  N [Armitage et al., 2009b]. Paul et al. [2009] similarly estimated total global historical PFOS emissions to air and water to be  $4.5 \times 10^2$  to  $2.7 \times 10^3$  Mg between 1970 and 2002. Indirect (atmospheric) PFOS inputs to the global oceans are thought to be smaller (5–230 Mg) based on work by Armitage et al. [2009a]. We find the high estimate of PFOS releases derived here is implausible based on these global production constraints [Armitage et al., 2009a; Paul et al., 2009].

Figure 2a compares modeled surface seawater (10 m) concentrations for the year 2010 based on the median scenario for PFOS releases (Figure 1) with observed surface seawater concentrations between 2009 and 2011. Relatively high concentrations are apparent next to continental source regions in eastern North America and the North Sea, and relatively lower levels are observed in the eastern subtropical region (Sargasso Sea). We divided the North Atlantic Ocean into the biogeographical provinces characterized by Longhurst [2007] to

developing areas [Filipovic et al., 2013; Xie et al., 2013]. We scaled temporal changes in population-based inputs using global historical release inventories in the same manner as other regions [Armitage et al., 2009b; Wang et al., 2014a].

We assumed all riverine PFOS will enter the ocean within 1 year except for systems where flow is mediated by the presence of a large inland water body (i.e., the St. Lawrence River/Lake Ontario, the Nelson River/Lake Winnipeg, and the Danish Straits/Baltic Sea). We estimated transport times for these systems by calibrating the

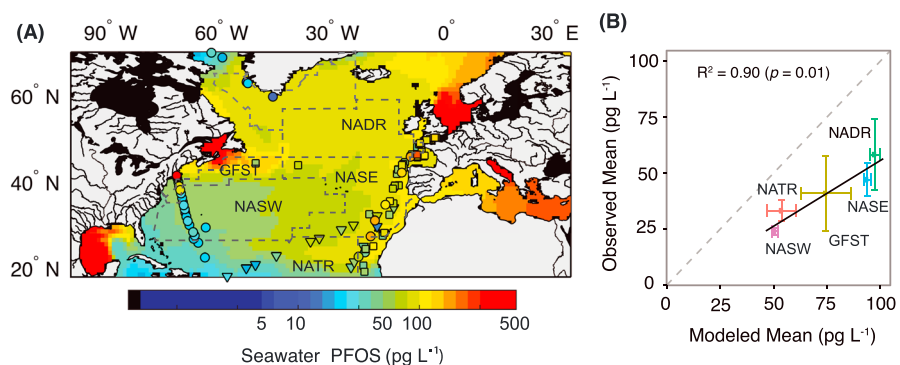


**Figure 2.** Modeled and observed surface seawater PFOS concentrations ( $\text{pg L}^{-1}$ ) in the North Atlantic Ocean. (a) The modeled surface (10 m) seawater concentrations for 2010 compared to observations for 2009–2011. (b) The modeled and observed PFOS concentrations grouped by Longhurst Biogeographical Provinces [Longhurst, 2007], where error bars indicate standard error around the mean for both the model and observations. Grey dashed line indicates 1:1 fit between modeled and observed surface water concentrations. Regression slope indicates the median release scenario (Figure 1) results in a model bias relative to surface water PFOS observations of 75%. Modeled surface water concentrations capture 90% of the observed variability across biogeographical provinces [Longhurst, 2007]. NADR = North Atlantic Drift Province [Ahrens et al., 2009a, 2010b; Benskin et al., 2012], GFST = Gulf Stream Province, NASW = North Atlantic Subtropical Province (west), NASE = North Atlantic Subtropical Province (east), and NATR = North Atlantic Tropical Gyral Province. Surface PFOS measurements are from Ahrens et al. [2009a, 2009b, 2010b]; Benskin et al. [2012], Gonzalez-Gaya et al. [2014], and Zhao et al. [2012].

assess performance of the model in different regions. We do not consider coastal monitoring data because the model is not intended to capture the fine-scale circulation and dynamics of inland seas and estuaries.

Modeled seawater concentrations capture most of the variability in the observed data ( $R^2 = 0.90, p = 0.01$ ) across biogeographical provinces (Figure 2b). The grey dashed line in Figure 2b indicates perfect agreement between measured and modeled results, and the regression relationship indicates that the model has a high mean bias of 75% relative to observations for all regions. Measured PFOS concentrations are lower in the western portion of the North Atlantic Subtropical Gyral Province (NASW) in the Sargasso Sea, and the southern North Atlantic Tropical Gyral Province (NATR), than those in the eastern North Atlantic Subtropical Gyral Province (NASE). The model successfully captures these differences. Only two surface water measurements ranging from  $<10 \text{ pg L}^{-1}$  to  $59 \text{ pg L}^{-1}$  are available for the Gulf Stream Province (GFST) [Ahrens et al., 2010a; Benskin et al., 2012]. The model shows large ranges in PFOS concentrations in the Gulf Stream due to a plume of PFOS enriched seawater transported offshore (Figure 2a). Modeled seawater PFOS concentrations are elevated ( $>50 \text{ pg L}^{-1}$ ) in the North Atlantic Drift Province (NADR) and the subarctic regions below Greenland. Surface observations near the European shelf appear to support this spatial pattern (Figure 2).

Yamashita et al. [2008] collected five vertical profiles from the Labrador Sea and mid-Atlantic Ocean in 2004, which we compare to modeled seawater PFOS concentrations from the same regions and year. The median PFOS release scenario (solid red line in Figure 3) reasonably captures observed surface enrichment at stations AO2, AO4, and AO5 and depletion at depth (Figure 3). However, the median emissions scenario overestimates PFOS concentrations throughout the vertical profiles (Figure 3), which is consistent with model bias identified for surface water concentrations (Figure 2b). The model does not capture some of the fine-scale vertical variability at stations AO3–AO5 due to its coarse resolution ( $1^\circ \times 1^\circ$ ). The low release scenario from Figure 1 (dashed red line in Figure 3) better matches the observed magnitude of seawater PFOS concentrations in the Labrador Sea but underestimates those in the mid-Atlantic.

This analysis suggests that a mean model bias correction of 75% based on Figure 2b is appropriate for all results. Therefore, cumulative PFOS inputs to the North Atlantic Ocean of  $2.4 \times 10^3 \text{ Mg}$  are most consistent with available observational constraints from seawater measurements. Releases of this magnitude produce mean modeled surface water (10 m) concentrations of  $39 \pm 14 \text{ pg L}^{-1}$  in 2010 compared to an observed value across all offshore sampling locations of  $43 \pm 21 \text{ pg L}^{-1}$  between 2009 and 2011. Hereon, this bias corrected release scenario is used for all modeling and mass budget calculations.

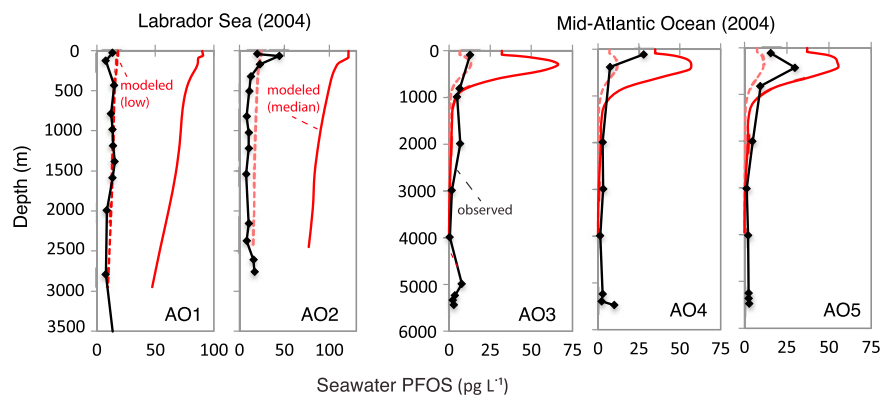


**Figure 3.** Comparison of modeled and observed vertical profiles of PFOS measured in the Labrador Sea and mid-Atlantic Ocean by Yamashita *et al.* [2008]. Observations are shown in black, and model scenarios are in red based on the median (solid line) and low (dashed line) PFOS release estimates shown in Figure 1.

## 5. Model Uncertainty and Sensitivity Analysis

For all ocean inputs, we conducted sensitivity analyses allowing for additional lag times of 2, 5, and 10 years between PFOS distribution in products and releases from watersheds to the ocean (Figure S7). Some studies have suggested that there may be a substantial lag between wastewater PFOS releases to aquatic systems and transport to marine areas due to slow transport in groundwater [Filipovic *et al.*, 2013]. We find introducing an additional lag exacerbates overestimates for recently measured surface seawater concentrations (Figures 2b and 3). Thus, we retain the base assumption that most PFOS releases in wastewater will be transported to the ocean within 1 year.

We consider uncertainty in the empirically measured partition coefficient for PFOS using sensitivity analysis on the upper and lower bounds reported in the literature ( $\log K_{oc} = 2.4$  to  $3.8$ ) [Ahrens *et al.*, 2011; Ferrey *et al.*, 2012]. Results of our simulation suggest that the mass of vertically transported PFOS in the ocean associated with settling particles is negligible compared to that from lateral and vertical ocean circulation (Figure S8). Modeled concentrations of PFOS bound to particles (Figure S8) are consistent with limited measurements that were all  $<10 \text{ pg L}^{-1}$  [Ahrens *et al.*, 2009a]. We examined the sensitivity of this finding to the range in partition coefficients reported in the literature. The maximum  $\log K_{oc}$  value reported in prior work is 3.8 [Ahrens *et al.*, 2011], compared to the value of 2.6 [Higgins and Luthy, 2006] specified in our base simulation. This does not change our initial finding as the fraction of particle bound PFOS in seawater is negligible across expected ranges of  $K_{oc}$  and potential POC concentrations in seawater (Figure S9). Previous studies that considered PFOS fluxes associated with settling of suspended particles in isolation suggest this may be a substantial oceanic transport process [Sanchez-Vidal *et al.*, 2015]. Our model results indicate this is not the case for the North Atlantic.

## 6. Spatial Distribution of PFOS in Seawater

The major surface currents in the Atlantic Ocean result in predominantly eastern and northern transport of coastal PFOS pollution sources toward the Subarctic (Figure 4). Surface water PFOS concentrations in 1980 and 2000 varied by more than an order of magnitude in PFOS enriched seawater plumes from the St. Lawrence River, Florida Current, and North Sea (Figure 4a). The Gulf Stream transports PFOS entrained in the Florida Current into the central and eastern Atlantic Ocean, where it merges with the North Atlantic Current (NAC) and diverges both north and east [Pickard and Emery, 1990]. This is visible in Figures 4a and 4b by offshore dilution and diffusion north and east of elevated PFOS concentrations in the Gulf Stream. These results help to explain the relatively lower PFOS concentrations measured in seawater from the western part of the North Atlantic Subtropical Gyral Province (NASW, Figure 2).

Transport patterns for PFOS enriched surface waters (Figure 2) imply the North Atlantic is a large source to the Arctic. North Atlantic seawater enters the Arctic at multiple depths. This circulation is critical for transfer of heat into polar regions and meridional overturning of the ocean [Askenov *et al.*, 2010]. PFOS discharges

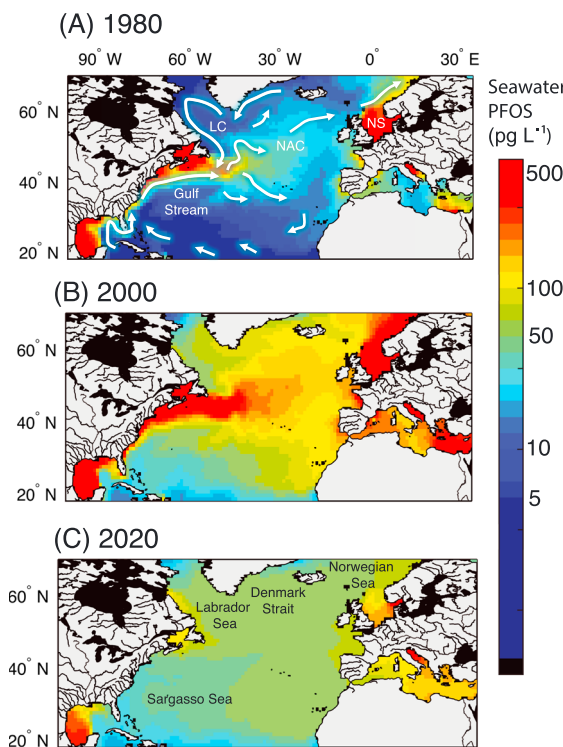


**Figure 4.** Modeled temporal evolution of surface water (10 m) PFOS concentrations in the North Atlantic Ocean between 1980 and 2020. The model is forced with the median release scenarios from rivers and wastewater shown in Figure 1 and zero releases between 2010 and 2020, adjusted by the mean model bias of 75% shown in Figure 2. Major surface currents are shown as white arrows. NAC = North Atlantic Current, LC = Labrador Current, and NS = North Sea.

of PFOS to the ocean floor in this region (mean:  $12 \text{ pg L}^{-1}$  below 1000 m) based on the vertical profiles measured by Yamashita *et al.* [2008] in the Labrador Sea in 2004 (Figure 3). For vertical profiles collected by Yamashita *et al.* [2008] between  $25^{\circ}\text{N}$  and  $30^{\circ}\text{N}$  (Figure 3), seawater below 1000 m also contained detectable but lower levels of PFOS (generally  $<5 \text{ pg L}^{-1}$ , Figure 3). These water depths primarily contain NADW transported south and may have some influence from Mediterranean outflow [Pickard and Emery, 1990]. Rhein *et al.* [2015] reported the western Atlantic portion of NADW around these latitudes (in the Sargasso Sea) has an apparent age of around 30 years, which suggests an influence from surface inputs of PFOS in the early to middle 1970s.

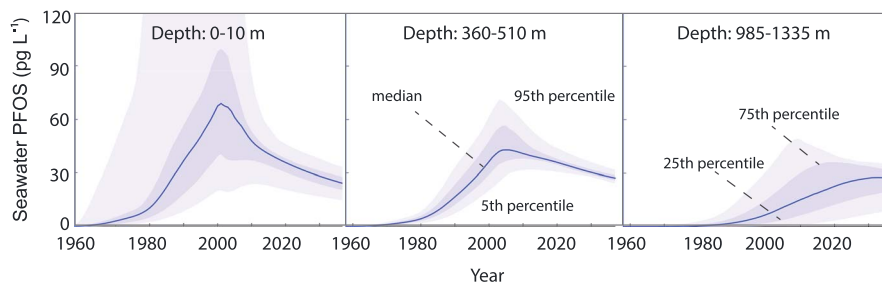
## 7. Temporal Changes in PFOS Concentrations and Mass Budgets for the North Atlantic

Figure 5 shows the temporal evolution of PFOS concentrations in seawater from the surface mixed layer (0–10 m), subsurface (360–510 m), and near the permanent thermocline (985–1335 m). Concentrations between 0 and 10 m depth peak in 2001 (basin-wide median:  $66 \text{ pg L}^{-1}$ ), 1 year after maximum releases from rivers and wastewater. Spatial heterogeneity in surface water concentrations is reflected by the wide variability in 95th percentile confidence intervals (CI) shown in Figure 5 (2001:  $9\text{--}633 \text{ pg L}^{-1}$ ) that become more homogeneous over time (2015:  $22\text{--}53 \text{ pg L}^{-1}$ ).

PFOS concentrations in subsurface seawater (365–510 m) are lower and less variable than surface waters due to dilution with lower concentration subsurface seawater (Figure 5). The lag time between peak releases (circa 2000) and peak subsurface concentrations (circa 2005,  $41 \text{ pg L}^{-1}$ , 95th CI: 27–66) at these depths is 2–3 years. This likely reflects strong winter convection in the subpolar North Atlantic, which results in

from the North Sea (Figure 4) are predominantly transported north into the Norwegian and Greenland Seas [Smith *et al.*, 2011]. Surface waters from this area enriched in PFOS become dense during winter cooling, sink, and form the lower limb of the North Atlantic Deep Water (NADW) that flows south as part of global thermohaline circulation [Pickard and Emery, 1990]. The Norwegian and Greenland Sea regions supply an estimated 80% of the NADW [Harvey and Theodorou, 1986; Pickard and Emery, 1990].

Similarly, surface waters entrained in the Labrador Current that captures PFOS discharges from the Hudson Bay sink in “convective chimneys” from the center of the Labrador Gyre [Clarke and Gascard, 1983] and are transported south in NADW primarily in the western Atlantic in the Deep Western Boundary Current (DWBC) [Rhein *et al.*, 2015]. Apparent ages of NADW determined from tracers around  $55^{\circ}\text{N}$  are generally less than a decade, even at depths greater than 3500 m [Doney and Bullister, 1992; Rhein *et al.*, 2015]. This explains the penetration



**Figure 5.** Modeled PFOS concentrations in North Atlantic Seawater ( $\text{pg L}^{-1}$ ) between  $20^{\circ}\text{N}$  and  $60^{\circ}\text{N}$  at different seawater depths based on the median PFOS release scenarios shown in Figure 1, adjusted for mean bias (75%). Shading indicates distributions of concentrations in different ocean regions with the median across the whole basin indicated as a solid line. Darker shading indicates 25th and 75th percentile modeled concentrations and 95th percentiles are shown as the lightest blue bounds.

mixing with subsurface waters up to  $\sim 600$  m depth [McCartney and Talley, 1982]. By 2015, median modeled concentrations declined to  $37 \text{ pg L}^{-1}$  and variability in ocean concentrations is much smaller than earlier years (95th CI: 30–47, Figure 5).

A longer lag after peak releases is observed for peak PFOS concentrations in deeper waters around the permanent thermocline (985–1335 m) (Figure 5). Modeled concentrations plateau in 2040 around a median of  $26 \text{ pg L}^{-1}$ . The effects of water mass circulation in different regions are evident in Figure 5, where the 95th percentile concentrations, representing more recently ventilated water masses, peaked in 2009 at  $47 \text{ pg L}^{-1}$  (a 9 year lag) and have declined since this time. By contrast, the 5th percentile of PFOS concentrations in the North Atlantic are continuing to slowly increase and are expected to reach  $9 \text{ pg L}^{-1}$  in 2040 (lag time more than three decades). Similar patterns have been reported for other pollutants in the North Atlantic such as lead (Pb), due to time required for subduction and ventilation of surface seawater into the thermocline [Wu and Boyle, 1997].

Cumulative PFOS inputs to the North Atlantic between 1958 and 2015 estimated in this study are  $2.4 \times 10^3 \text{ Mg}$ . The North Atlantic PFOS reservoir in 2015 was equivalent to approximately 60% of inputs in 2015 ( $1.4 \times 10^3 \text{ Mg}$ , Figure 6), with the remaining fractions lost to the Arctic Ocean (30%), tropical Atlantic plus other regions (10%). Over time, the mass distribution of PFOS has shifted toward deeper waters from  $>80\%$  in the upper ocean (top 1000 m) in 2000 to approximately 50% in 2015, consistent with Figure 5. This has important implications for reducing biological exposures as most marine life is found in the upper 1000 m of the ocean [Ryther, 1969].

Lifetimes of PFOS against losses (reservoir/gross losses) from this work range from 1 to 3 years (half-life:  $t_{1/2} = 1\text{--}2$  years) in the surface mixed layer of the North Atlantic to one to two decades in the deep ocean (Table 1). Loss processes are mainly internal circulation and outflow to the Arctic ( $>60^{\circ}\text{N}$ ), Mediterranean Sea, and the tropical Atlantic Ocean ( $<20^{\circ}\text{N}$ ) (Figure 6). By 2015, 85% of total losses from the Atlantic Ocean had been transported into the Arctic, with smaller outflow to other regions. Basin-wide lifetimes are shorter in 2000 than 2015, reflecting the entrainment of PFOS source regions in energetic currents in the ocean such as the Gulf Stream (Figure 4). Gonzalez-Gaya *et al.* [2014] estimated a 5.8 year half-life in the

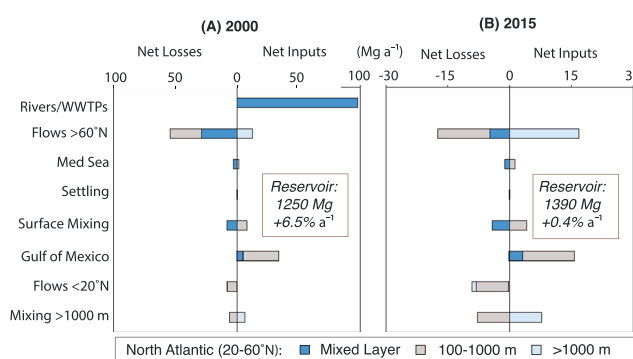


**Figure 6.** Mass flows of PFOS in the North Atlantic ( $\text{Mg a}^{-1}$ ) between  $20^{\circ}\text{N}$  and  $60^{\circ}\text{N}$  for the years 2000 (peak inputs) and 2015. Results are from the median release scenario (Figure 1) and adjusted for mean bias (75%).

**Table 1.** PFOS Reservoirs (Mg) in Surface, Middepth, and Deep Waters of the North Atlantic Ocean ( $20^{\circ}\text{N}$ – $60^{\circ}\text{N}$ ) in 2000 and 2015 and Lifetimes Against Losses ( $\tau, \text{a}^{-1}$ )

	2000	2015
<i>Reservoirs (Mg)</i>		
Surface mixed layer	380	95
Middepth (100–1000 m)	630	650
Deep (1000 m to bottom)	240	650
Full basin ( $20^{\circ}\text{N}$ – $60^{\circ}\text{N}$ )	1250	1390
<i>Lifetimes (<math>\text{a}^{-1}</math>)</i>		
Surface mixed layer	2.6	1.6
Middepth (100–1000 m)	4.0	4.7
Deep (1000 m to bottom)	13.9	20.9
Full basin ( $20^{\circ}\text{N}$ – $60^{\circ}\text{N}$ )	10.8	14.1

exposures since 2011 for fish and marine mammals that predominantly forage in the ocean surface mixed layer. Temporal changes are expected to be more variable for complex food webs with mixed prey items and biota that forage from deeper seawater such as North Atlantic pilot whales (*Globicephala melas*) that mainly consume squid between 400 and 700 m depth [Hoydal and Lastein, 1993; Li et al., 2015]. A reported increase in PFOS concentrations in pilot whale muscle between 1987 and the present is consistent with trends in middepth to thermocline waters shown in Figure 5 [Dassuncao et al., 2017].

## 8. Implications for PFOS Inputs to the Arctic Ocean

Figure 7 shows gross PFOS flows at different seawater depths into and out of the Arctic (above  $60^{\circ}\text{N}$ ) from the North Atlantic between 1958 and 2040. Most inputs to the Arctic Ocean are from middepth inflow (20–1000 m), which cumulatively accounted for  $1.1 \times 10^3$  Mg PFOS between 1958 and 2015 (surface inflow, 0–20 m = 60 Mg). Some of the North Atlantic inflow sank and mixed with deep water from the Arctic before traveling south, thereby reducing inputs to the high Arctic.

Circulation of PFOS transported beyond  $60^{\circ}\text{N}$  that returns south in deep water inflows (>1000 m depth, blue colors in Figure 7) cumulatively totaled  $4.1 \times 10^2$  Mg between 1958 and 2015 (Figure 7). NADW formation in the Labrador and Greenland Seas ( $44\text{--}65^{\circ}\text{W}$ ,  $50\text{--}65^{\circ}\text{N}$ ) between 1958 and 2015 resulted in  $4.8 \times 10^2$  Mg PFOS transported below 1000 m. We find 25% of this flux sinks below 1000 m south of  $60^{\circ}\text{N}$ , resulting in a total removal of  $5.3 \times 10^2$  Mg PFOS associated with Atlantic meridional overturning circulation (AMOC).

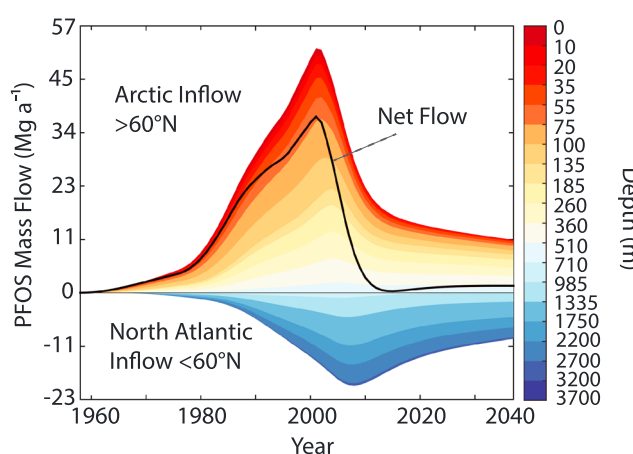


**Figure 7.** Modeled circulation of PFOS above and below  $60^{\circ}\text{N}$  at different seawater depths between 1958 and 2040. Deeper waters are indicated by blue, and surface waters are shown in shades of red, orange, and yellow. Solid black line indicates net flow, where positive numbers indicate flow above  $60^{\circ}\text{N}$  (into the Arctic region) and negative numbers indicate flow below  $60^{\circ}\text{N}$  (into the North Atlantic).

North Atlantic based on observations for another PFAS with the same number of carbon atoms. For seawater between 100 and 1000 m, modeled half-lives for PFOS in this study were approximately 3 years.

Variable lag times and vertical differences in seawater concentrations (Table 1 and Figure 5) help to explain mixed temporal trends in biological PFOS concentrations measured in the North Atlantic and Subarctic [Bossi et al., 2005; Butt et al., 2010; Dassuncao et al., 2017]. Our results imply declining PFOS

exposures since 2011 for fish and marine mammals that predominantly forage in the ocean surface mixed layer. Temporal changes are expected to be more variable for complex food webs with mixed prey items and biota that forage from deeper seawater such as North Atlantic pilot whales (*Globicephala melas*) that mainly consume squid between 400 and 700 m depth [Hoydal and Lastein, 1993; Li et al., 2015]. A reported increase in PFOS concentrations in pilot whale muscle between 1987 and the present is consistent with trends in middepth to thermocline waters shown in Figure 5 [Dassuncao et al., 2017].

*Rahmstorf et al., 2015; Rhein et al., 2015; Yashayaev, 2007]. These climate-driven changes thus have the potential to greatly increase the magnitude of bioaccumulative pollutants entering ecologically sensitive Arctic regions.*

## 9. Summary and Conclusions

We developed a new 3-D simulation for the fate of cumulative PFOS inputs ( $2.4 \times 10^3$  Mg) to the North Atlantic Ocean between 1958 and 2015. Results suggest concentrations in surface waters (upper 1000 m) reached maximum levels several years after peak global PFOS production (before 2005) but concentrations in the deep ocean will continue to rise until 2040. Modeled temporal changes in the North Atlantic (Figure 5) contrast previous work that suggested ocean concentrations will decline slowly in all PFOS source regions and will increase in remote regions for several decades [Armitage et al., 2009a]. The abrupt phase out of most chemical manufacturing of PFOS around the year 2000, its high stability in seawater, and limited transport associated with settling of suspended particles in the ocean water column reinforce its potential as a novel tracer of ocean circulation. Recent declines in PFOS concentrations in the upper ocean are important for protecting marine food webs known to bioaccumulate this deleterious compound [Dassuncao et al., 2017; Routti et al., 2016; Houde et al., 2011; Tomy et al., 2004].

In 2015, we estimate the North Atlantic (20–60°N) reservoir of PFOS to be  $1.4 \times 10^3$  Mg. Model results suggest  $7.3 \times 10^2$  Mg PFOS has entered the Arctic Ocean from the North Atlantic, and smaller amounts ( $2.9 \times 10^2$  Mg, Figure 6) have been transported to the tropical and southern Atlantic Ocean and other regions. When peak discharges were occurring, surface currents in the Atlantic Ocean transported PFOS from continental source regions to the Subarctic, explaining the large Arctic inputs. However, a large fraction of the PFOS that reached high latitudes became part of the NADW and was transported south in global thermohaline circulation. We estimate AMOC has cumulatively prevented  $5.3 \times 10^2$  Mg PFOS from entering the high Arctic since the onset of its production in 1958. Weakened AMOC in an era of rapidly changing climate is thus expected to increase the burden of persistent, bioaccumulative contaminants entering ecologically sensitive Arctic regions.

## Acknowledgments

Financial support for this work was provided by the U.S. National Science Foundation (PLR 1203496) and the Richard and Susan Smith Family Foundation. X.Z. received support from a Postdoctoral Fellowship from the Natural Sciences and Engineering Research Council of Canada. We acknowledge Global Runoff Data Centre (<http://www.bafg.de/>) and Socioeconomic Data and Applications Center (<http://sedac.ciesin.columbia.edu/>) for GIS data. We thank D.C.G. Muir, S. Fraser, S.A. Smyth, P. Guerra (Environment Canada), J.M. Armitage (University of Toronto), I. Cousins (Stockholm University), A. Pistocchi, and R. Loos (Joint Research Centre of the European Commission), for valuable communications during this study. We thank Stephanie Dutkiewicz (MIT) for assistance with the MITgcm.

## References

- 3M (2000), Sulfonated perfluorochemicals: Life-cycle waste stream estimates—Final report for 3M specialty materials, 1063–1072. [Available at <http://www.chemicalindustryarchives.org/dirtysecrets/scotchgard/pdfs/1226-0681.pdf>, accessed February 2014.]  
Ahrens, L., J. L. Barber, Z. Y. Xie, and R. Ebinghaus (2009a), Longitudinal and latitudinal distribution of perfluoroalkyl compounds in the surface water of the Atlantic Ocean, *Environ. Sci. Technol.*, 43(9), 3122–3127.  
Ahrens, L., S. Felizeter, and R. Ebinghaus (2009b), Spatial distribution of polyfluoroalkyl compounds in seawater of the German Bight, *Chemosphere*, 76(2), 179–184.  
Ahrens, L., W. Gerwinski, N. Theobald, and R. Ebinghaus (2010a), Sources of polyfluoroalkyl compounds in the North Sea, Baltic Sea and Norwegian Sea: Evidence from their spatial distribution in surface water, *Mar. Pollut. Bull.*, 60(2), 255–260.  
Ahrens, L., Z. Y. Xie, and R. Ebinghaus (2010b), Distribution of perfluoroalkyl compounds in seawater from Northern Europe, Atlantic Ocean, and Southern Ocean, *Chemosphere*, 78(8), 1011–1016.  
Ahrens, L., L. W. Y. Yeung, S. Taniyasu, P. K. S. Lam, and N. Yamashita (2011), Partitioning of perfluorooctanoate (PFOA), perfluorooctane sulfonate (PFOS) and perfluorooctane sulfonamide (PFOSA) between water and sediment, *Chemosphere*, 85(5), 731–737.  
Armitage, J. M., M. MacLeod, and I. T. Cousins (2009a), Modeling the global fate and transport of perfluorooctanoic acid (PFOA) and perfluorooctanoate (PFO) emitted from direct sources using a multispecies mass balance model, *Environ. Sci. Technol.*, 43(4), 1134–1140.  
Armitage, J. M., U. Schenker, M. Scheringer, J. W. Martin, M. Macleod, and I. T. Cousins (2009b), Modeling the global fate and transport of perfluorooctane sulfonate (PFOS) and precursor compounds in relation to temporal trends in wildlife exposure, *Environ. Sci. Technol.*, 43(24), 9274–9280.  
Askenov, Y., S. Bacon, A. C. Coward, and A. J. G. Nurser (2010), The North Atlantic inflow to the Arctic Ocean: High resolution model study, *J. Mar. Syst.*, 79, 1–22.  
Benskin, J. P., et al. (2012), Perfluoroalkyl acids in the Atlantic and Canadian Arctic Oceans, *Environ. Sci. Technol.*, 46, 5815–5823.  
Bossi, R., F. F. Riget, R. Dietz, C. Sonne, P. Fauser, M. Dam, and K. Vorkamp (2005), Preliminary screening of perfluorooctane sulfonate (PFOS) and other fluorocompounds in fish, birds and marine mammals from Greenland and the Faroe Islands, *Environ. Pollut.*, 136(2), 323–329.  
Boulanger, B., J. Vargo, J. L. Schnoor, and K. C. Hornbuckle (2004), Evaluation of perfluorooctane surfactants in a wastewater treatment system and in a commercial surface protection product, *Environ. Sci. Technol.*, 39, 5524–5530.  
Buser, A., and L. Morf (2009), Substance flow analysis of PFOS and PFOA, in *Perfluorinated Surfactants Perfluorooctanesulfonate (PFOS) and Perfluorooctanoic Acid (PFOA) in Switzerland*, Federal Office for the Environment (FOEN), Berne, Switz.  
Butt, C. M., U. Berger, R. Bossi, and G. T. Tomy (2010), Levels and trends of poly- and perfluorinated compounds in the arctic environment, *Sci. Total Environ.*, 408, 2936–2965.  
Campbell, T. Y., C. D. Vecitis, B. T. Mader, and M. R. Hoffmann (2009), Perfluorinated surfactant chain-length effects on sonochemical kinetics, *J. Phys. Chem. A*, 113(36), 9834–9842.  
Center for International Earth Science Information Network, Columbia University, United Nations Food Agriculture Programme, and Centro Internacional de Agricultura Tropical (2005), Gridded Population of the World, version 3 (GPWv3): Population count grid, Future Estimates, edited, NASA Socioeconomic Data and Applications Center (SEDAC), Palisades, N. Y.

- Cheng, J., E. Psillakis, M. R. Hoffmann, and A. J. Colussi (2009), Acid dissociation versus molecular association of perfluoroalkyl oxoacids: environmental implications, *J. Phys. Chem. A*, 113(29), 8152–8156.
- Clarke, R. A., and J. Gascard (1983), The formation of Labrador Sea Water. Part 1: Large-scale processes, *J. Phys. Oceanogr.*, 13, 1764–1778.
- Dassuncao, C., X. C. Hu, X. Zhang, R. Bossi, M. Dam, B. Mikkelsen, and E. M. Sunderland (2017), Temporal shifts in poly- and perfluoroalkyl substances (PFASs) in North Atlantic pilot whales indicate large contribution of atmospheric precursors, *Environ. Sci. Technol.*, 51(8), 4512–4521.
- D'eon, J. C., P. W. Crozier, V. I. Furdui, E. J. Reiner, E. L. Libelo, and S. A. Mabury (2009), Perfluorinated phosphonic acids in Canadian surface waters and wastewater treatment plant effluent: Discovery of a new class of perfluorinated acids, *Environ. Toxicol. Chem.*, 28, 2101–2107.
- Doney, S. C., and J. L. Bullister (1992), A chlorofluorocarbon section in the eastern North Atlantic, *Deep Sea Res. Part A*, 39(11–12), 1857–1883.
- Dutkiewicz, S., M. J. Follows, and J. G. Bragg (2009), Modeling the coupling of ocean ecology and biogeochemistry, *Global Biogeochem. Cycles*, 23, GB4017, doi:10.1029/2008GB003405.
- Earnshaw, M. R., A. G. Paul, R. Loos, S. Tavazzi, B. Paracchini, M. Scheringer, K. Hungerbuhler, K. C. Jones, and A. J. Sweetman (2014), Comparing measured and modelled PFOS concentrations in a UK freshwater catchment and estimating emission rates, *Environ. Int.*, 70C, 25–31.
- Environment Canada (2009), Municipal water and wastewater survey. [Available at <http://www.ec.gc.ca/eau-water/default.asp?lang=En&n=ED7C2D33-31>, accessed March 2014.]
- Erickson, M., M. Ferrey, P. Hoff, L. Solem, and S. Streets (2009), PFCs in Minnesota's ambient environment: 2008 progress report. Minnesota Pollution Control Agency. [Available at <http://www.pca.state.mn.us/index.php/view-document.html?gid=2855>, accessed February 2014.]
- Ferrey, M. L., J. T. Wilson, C. Adair, C. M. Su, D. D. Fine, X. Y. Liu, and J. W. Washington (2012), Behavior and fate of PFOA and PFOS in sandy aquifer sediment, *Ground Water Monit. R.*, 32(4), 63–71.
- Filipovic, M., U. Berger, and M. S. McLachlan (2013), Mass balance of perfluoroalkyl acids in the Baltic Sea, *Environ. Sci. Technol.*, 47(9), 4088–4095.
- Furdui, V. I., P. W. Crozier, E. J. Reiner, and S. A. Mabury (2008), Trace level determination of perfluorinated compounds in water by direct injection, *Chemosphere*, 73(1), S24–S30.
- Furl, C. V., C. A. Meredith, M. J. Strynar, and S. F. Nakayama (2011), Relative importance of wastewater treatment plants and non-point sources of perfluorinated compounds to Washington State rivers, *Sci. Total Environ.*, 409(15), 2902–2907.
- Fisher, J., M. Visbeck, R. Zantopp, and N. Nunes (2010), Interannual to decadal variability of outflow from the Labrador Sea, *Geophys. Res. Lett.*, 37, L24610, doi:10.1029/2010GL045321.
- Global Runoff Data Centre (2007), Major river basins of the world, The Global Runoff Data Centre, D-56002 Koblenz, Germany. [Available at <http://www.bafg.de/GRDC/>, accessed April 2014.]
- Gonzalez-Gaya, B., J. Dachs, J. Roscales, G. Caballero, and B. Jimenez (2014), Perfluorinated substances in the global tropical and subtropical surface oceans, *Environ. Sci. Technol.*, 48, 13,076–13,084.
- Guerra, P., M. Kim, L. Kinsman, T. Ng, M. Alae, and S. A. Smyth (2014), Parameters affecting the formation of perfluoroalkyl acids during wastewater treatment, *J. Hazard. Mater.*, 272, 148–154.
- Harvey, J., and A. Theodorou (1986), The circulation of Norwegian Sea overflow water in the eastern North Atlantic, *Oceanol. Acta*, 9, 393–402.
- Higgins, C. P., and R. G. Luthy (2006), Sorption of perfluorinated surfactants on sediments, *Environ. Sci. Technol.*, 40(23), 7251–7256.
- Houde, M., A. O. De Silva, D. C. G. Muir, and R. J. Letcher (2011), Monitoring of perfluorinated compounds in aquatic biota: An updated review, *Environ. Sci. Technol.*, 45, 7962–7973.
- Hoydal, K., and L. Lastein (1993), Analysis of Faroese catches of pilot whales (1709–1992), in relation to environmental variations, in *Biology of Northern Hemisphere Pilot Whales*, edited by G. P. Donovan, C. H. Lockyer, and A. R. Martin, pp. 89–106, International Whaling Commission, Cambridge, U. K.
- Land, M., C. A. de Wit, I. T. Cousins, D. Herzke, J. Johansson, and J. W. Martin (2015), What is the effect of phasing out long-chain per- and polyfluoroalkyl substances on the concentrations of perfluoroalkyl acids and their precursors in the environment? A systematic review protocol, *Environ. Evidence*, 4, 3.
- Li, M., L. S. Sherman, J. D. Blum, P. Grandjean, B. Mikkelsen, P. Weihe, E. M. Sunderland, and J. P. Shine (2015), Assessing sources of human methylmercury exposure using stable mercury isotopes, *Environ. Sci. Technol.*, 48, 8800–8806.
- Loganathan, B. G., K. S. Sajwan, E. Sinclair, K. S. Kumar, and K. Kannan (2007), Perfluoroalkyl sulfonates and perfluorocarboxylates in two wastewater treatment facilities in Kentucky and Georgia, *Water Res.*, 41(20), 4611–4620.
- Longhurst, A. R. (2007), *Ecological Geography of the Sea*, 2nd ed., Academic Press, Elsevier, San Diego, Calif.
- Lohmann, R., E. Jurado, H. A. Dijkstra, and J. Dachs (2013), Vertical eddy diffusion as a key mechanism for removing perfluorooctanoic acid (PFOA) from the global surface oceans, *Environ. Pollut.*, 179, 88–94.
- Marshall, J., C. Hill, L. Perelman, and A. Adcroft (1997), Hydrostatic, quasi-hydrostatic, and nonhydrostatic ocean modeling, *J. Geophys. Res.*, 102(C3), 5733–5752.
- McCartney, M., and L. D. Talley (1982), The subpolar model water of the North Atlantic Ocean, *J. Phys. Oceanogr.*, 12, 1169–1188.
- Muir, D., and R. Lohmann (2013), Water as a new matrix for global assessment of hydrophilic POPs, *TrAC, Trends Anal. Chem.*, 46, 162–172.
- Paul, A. G., K. C. Jones, and A. J. Sweetman (2009), A first global production, emission and environmental inventory for perfluorooctane sulfonate, *Environ. Sci. Technol.*, 43(2), 386–392.
- Pickard, G. L., and W. J. Emery (1990), *Descriptive Physical Oceanography*, 5th ed., p. 320, Butterworth-Heinemann, Woburn, Mass.
- Pistocchi, A., and R. Loos (2009), A map of European emissions and concentrations of PFOS and PFOA, *Environ. Sci. Technol.*, 43(24), 9237–9244.
- Plumlee, M. H., J. Larabee, and M. Reinhard (2008), Perfluorochemicals in water reuse, *Chemosphere*, 72(10), 1541–1547.
- Prevedouros, K., I. T. Cousins, R. C. Buck, and S. H. Korzeniowski (2006), Sources, fate and transport of perfluorocarboxylates, *Environ. Sci. Technol.*, 40(1), 32–44.
- Rahmstorf, S., J. E. Box, G. Feulner, M. E. Mann, A. Robinson, S. Rutherford, and E. J. Schaffernicht (2015), Exceptional twentieth-century slowdown in Atlantic Ocean overturning circulation, *Nat. Clim. Chang.*, 5, 475–480.
- Rayne, S., and K. Forest (2009), Perfluoroalkyl sulfonic and carboxylic acids: A critical review of physicochemical properties, levels and patterns in waters and wastewaters, and treatment methods, *J. Environ. Sci. Health. Part A Toxic/Hazard. Subst. Environ. Eng.*, 44, 1145–1199.
- Rhein, M., D. Kieke, and R. Steinfield (2015), Advection of North Atlantic Deep Water from the Labrador Sea to the southern hemisphere, *J. Geophys. Res. Oceans*, 120, 2471–2487, doi:10.1002/2014JC010605.
- Routti, H., G. W. Gabrielsen, D. Herzke, K. M. Kovacs, and C. Lydersen (2016), Spatial and temporal trends in perfluoroalkyl substances (PFASs) in ringed seals (*Pusa hispida*) from Svalbard, *Environ. Pollut.*, 214, 230–238.
- Ryther, J. H. (1969), Photosynthesis and fish production in the sea, *Science*, 166(3901), 72–76.

- Sanchez-Vidal, A., M. Llorca, M. Farre, M. Canals, and D. Barcelo (2015), Delivery of unprecedented amounts of perfluoroalkyl substances towards the deep-sea, *Sci. Total Environ.*, 526, 41–48.
- Schenker, U., M. Scheringer, M. Macleod, J. W. Martin, I. T. Cousins, and K. Hungerbuhler (2008), Contribution of volatile precursor substances to the flux of perfluorooctanoate to the Arctic, *Environ. Sci. Technol.*, 42, 3710–3716.
- Scott, B. F., C. Spencer, E. Lopez, and D. C. G. Muir (2009), Perfluorinated alkyl acid concentrations in Canadian rivers and creeks, *Water Qual. Res. J. Can.*, 44(3), 263–277.
- Schlitz, M. M., D. F. Barofsky, and J. A. Field (2006), Quantitative determination of fluorinated alkyl substances by large-volume-injection liquid chromatography tandem mass spectrometry—Characterization of municipal wastewater, *Environ. Sci. Technol.*, 40(1), 289–295.
- Smith, J. N., F. A. McLaughlin, W. M. J. Smethie, B. S. Moran, and K. Lepore (2011), Iodine-129,  $^{137}\text{Cs}$ , and CFC-11 tracer transit time distributions in the Arctic Ocean, *J. Geophys. Res.*, 116, C04024, doi:10.1029/2010JC006471.
- Stemmler, I., and G. Lammel (2010), Pathways of PFOA to the Arctic: Variabilities and contributions of oceanic currents and atmospheric transport and chemistry sources, *Atmos. Chem. Phys.*, 10, 9965–9980.
- Tomy, G. T., W. Budakoeski, T. Halldorson, P. A. Helm, G. A. Stern, K. Friesen, K. Pepper, S. A. Tittlemier, and A. T. Fisk (2004), Fluorinated organic compounds in an Eastern Arctic marine food web, *Environ. Sci. Technol.*, 38, 6475–6481.
- U.S. Environmental Protection Agency (EPA) (2008), Databased associated with the Clean Watersheds Needs Survey (CWNS) report to congress. [Available at <http://ofmpub.epa.gov/portal/page/portal/CWNS%20Reports/download>, accessed March 2014.]
- Vecitis, C. D., H. Park, J. Cheng, B. T. Mader, and M. R. Hoffmann (2008), Kinetics and mechanism of the sonolytic conversion of the aqueous perfluorinated surfactants, perfluorooctanoate (PFOA), and perfluorooctane sulfonate (PFOS) into inorganic products, *J. Phys. Chem. A*, 112(18), 4261–4270.
- Wang, Z., I. T. Cousins, M. Scheringer, R. C. Buck, and K. Hungerbuhler (2014a), Global emission inventories for C4–C14 perfluoroalkyl carboxylic acid (PFCA) homologues from 1951 to 2030, Part 1: Production and emissions from quantifiable sources, *Environ. Int.*, 70, 62–75.
- Wang, Z., I. T. Cousins, M. Scheringer, R. C. Buck, and K. Hungerbuhler (2014b), Global emission inventories for C4–C14 perfluoroalkyl carboxylic acid (PFCA) homologues from 1951 to 2030, Part II: The remaining pieces of the puzzle, *Environ. Int.*, 69, 166–176.
- Wang, Z., I. T. Cousins, and M. Scheringer (2015), Comment on "The environmental photolysis of perfluorooctanesulfonate, perfluorooctanoate, and related fluorochemicals", *Chemosphere*, 122, 301–303.
- Wang, Z., J. C. DeWitt, C. P. Higgins, and I. T. Cousins (2017), A never-ending story of per- and polyfluoroalkyl substances (PFASs)?, *Environ. Sci. Technol.*, 51(5), 2508–2518.
- Wania, F. (2007), A global mass balance analysis of the source of perfluorocarboxylic acids in the Arctic Ocean, *Environ. Sci. Technol.*, 41(13), 4529–4535.
- Wu, J., and E. A. Boyle (1997), Lead in the western North Atlantic Ocean: Completed response to leaded gasoline phaseout, *Geochim. Cosmochim. Acta*, 61(15), 3279–3283.
- Wunsch, C., and P. Heimbach (2007), Practical global oceanic state estimation, *Phys. D*, 230(1–2), 197–208.
- Xie, S. W., Y. L. Lu, T. Y. Wang, S. J. Liu, K. Jones, and A. Sweetman (2013), Estimation of PFOS emission from domestic sources in the eastern coastal region of China, *Environ. Int.*, 59, 336–343.
- Yamashita, N., S. Taniyasu, G. Petrick, S. Wei, T. Gamo, P. K. S. Lam, and K. Kannan (2008), Perfluorinated acids as novel chemical tracers of global circulation of ocean waters, *Chemosphere*, 70(7), 1247–1255.
- Yashayev, I. (2007), Hydrographic changes in the Labrador Sea, 1960–2005, *Prog. Oceanogr.*, 73, 242–276.
- Zareitalabad, P., J. Siemens, M. Hamer, and W. Amelung (2013), Perfluorooctanoic acid (PFOA) and perfluorooctanesulfonic acid (PFOS) in surface waters, sediments, soils and wastewater—A review on concentrations and distribution coefficients, *Chemosphere*, 91(6), 725–732.
- Zhang, L., J. G. Liu, J. X. Hu, C. Liu, W. G. Guo, Q. Wang, and H. Wang (2012), The inventory of sources, environmental releases and risk assessment for perfluorooctane sulfonate in China, *Environ. Pollut.*, 165, 193–198.
- Zhang, X., R. Lohmann, C. Dassuncao, X. C. Hu, A. K. Weber, C. D. Vecitis, and E. M. Sunderland (2016), Source attribution of poly and perfluoroalkyl substances (PFASs) in surface waters from Rhode Island and the New York Metropolitan Area, *Environ. Sci. Technol. Lett.*, 3(9), 316–321.
- Zhao, Z., Z. Y. Xie, A. Moller, R. Sturm, J. H. Tang, G. Zhang, and R. Ebinghaus (2012), Distribution and long-range transport of polyfluoroalkyl substances in the Arctic, Atlantic Ocean and Antarctic coast, *Environ. Pollut.*, 170, 71–77.



*Global Biogeochemical Cycles*

Supporting Information for:

**North Atlantic deep water formation inhibits high Arctic contamination by  
continental perfluorooctane sulfonate (PFOS) discharges**

Xianming Zhang<sup>a,b</sup>, Yanxu Zhang<sup>a</sup>, Clifton Dassuncao<sup>a,b</sup>, Rainer Lohmann<sup>c</sup>, and  
Elsie M. Sunderland<sup>a,b</sup>

<sup>a</sup> Harvard John A. Paulson School of Engineering and Applied Science, Harvard University,  
Cambridge, Massachusetts, USA

<sup>b</sup> Department of Environmental Health, Harvard T. H. Chan School of Public Health, Boston,  
Massachusetts, USA

<sup>c</sup> Graduate School of Oceanography, University of Rhode Island, Narragansett, RI, USA

## **Contents of this file**

### **Section 1: Supplementary information on PFOS release inventory**

**Figure S1.** PFOS discharges from major rivers in Europe in 2006-2007.

**Table S1.** Review of measured PFOS concentrations in effluents of wastewater treatment plants in North America.

**Figure S2.** Relationship between wastewater flow rates ( $m^3 d^{-1}$ ) and population in Canada and the U.S.

**Figure S3.** Relationships between population served by wastewater treatment plants (WWTPs) and PFOS discharges for Canada and the U.S.

**Figure S4.** Direct PFOS discharges in wastewater to North America estuaries ca. 2010.

**Figure S5.** PFOS discharges ( $kg a^{-1}$ ) in 2010 from rivers in North America to the ocean.

**Table S2.** Direct PFOS discharges to estuaries ( $kg a^{-1}$ ) from wastewater treatment plants ( $> 1 kg a^{-1}$ ) in Canada and the U.S. ca. 2010.

**Table S3.** Estimated 2009-2010 PFOS discharges  $> 2 kg a^{-1}$  from watersheds to the oceans.

**Figure S6.** Relationships between measured PFOS and population in Northern and Eastern European wastewater sampled in 2009-2010.

**Table S4.** Estimated time-lags in PFOS inputs to the ocean from rivers with flows mediated by large water bodies.

### **Section 1: Supplementary modeling results**

**Figure S7.** Sensitivity analysis on the effect of PFOS retention over the continent on modeled concentration in surface seawater in 2000 (peak release year) and 2010.

**Figure S8.** Comparison of concentrations and transport of particle-bound and dissolved PFOS.

**Figure S9.** Modeled concentrations of particle-bound PFOS (pg/L) in 2010 in the North Atlantic Ocean.

**Figure S10.** Influence of organic carbon normalized particle/water distribution coefficient ( $K_{oc}$ ) on particle-bound fraction of PFOS.

## **Introduction**

The Supporting Information contains four tables, and ten figures.

**Section 1: Supplementary information on release inventory for PFOS from wastewater treatment plants and rivers**

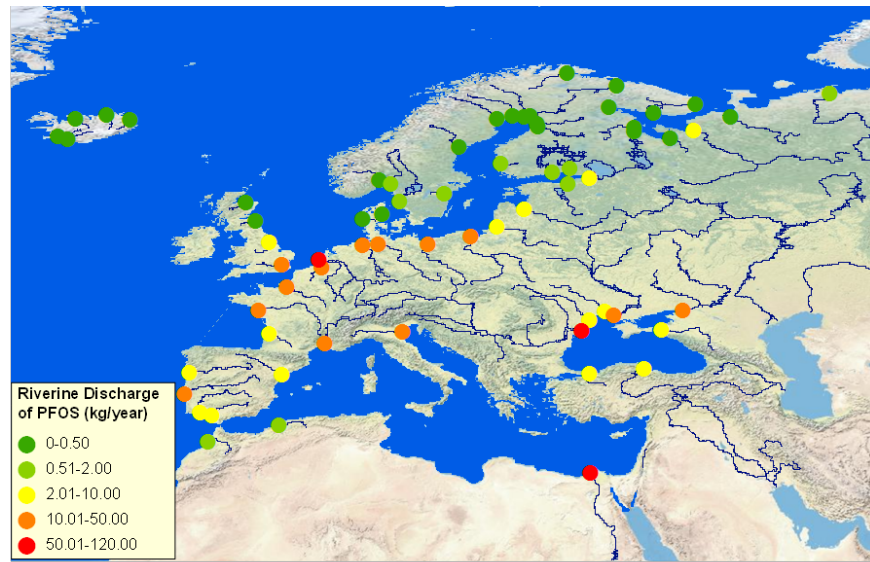


**Figure S1.** PFOS discharges from major rivers in Europe in 2006-2007 estimated based on the regression relationship with catchment population developed by *Pistocchi and Loos [2009]*.

**Table S1.** Review of measured PFOS concentrations in effluents of wastewater treatment plants in North America

a) United States Data

Sampling Year	Sampling Location	PFOS in effluent (ng L <sup>-1</sup> )	Reference
2004	Iowa, USA	26 ± 2.0	Boulanger <i>et al.</i> , 2005
2004	Oregon, USA	15 – 34	Schultz <i>et al.</i> , 2006
2005	Georgia, USA	13	Loganathan, <i>et al.</i> , 2007
2005	Georgia, USA	9	Loganathan, <i>et al.</i> , 2007
2005	Georgia, USA	2	Loganathan, <i>et al.</i> , 2007
2005	Kentucky, USA	14	Loganathan, <i>et al.</i> , 2007
2005	Kentucky, USA	8	Loganathan, <i>et al.</i> , 2007
2005	Kentucky, USA	13	Loganathan, <i>et al.</i> , 2007
2005	Kentucky, USA	28	Loganathan, <i>et al.</i> , 2007
2007	California, USA	38	Plumlee <i>et al.</i> , 2008
2007	California, USA	190	Plumlee <i>et al.</i> , 2008
2007	California, USA	20	Plumlee <i>et al.</i> , 2008
2007	California, USA	42	Plumlee <i>et al.</i> , 2008
2007	Minnesota, USA	< 4.91	Streets, 2008
2007	Minnesota, USA	9.46	Streets, 2008
2007	Minnesota, USA	< 4.91	Streets, 2008
2007	Minnesota, USA	< 10.0	Streets, 2008
2007	Minnesota, USA	45.00	Streets, 2008
2007	Minnesota, USA	< 5.17	Streets, 2008
2007	Minnesota, USA	8.02	Streets, 2008
2007	Minnesota, USA	< 5.25	Streets, 2008
2007	Minnesota, USA	< 4.95	Streets, 2008
2007	Minnesota, USA	< 5.22	Streets, 2008
2007	Minnesota, USA	32.50	Streets, 2008
2007	Minnesota, USA	< 5.16	Streets, 2008
2007	Minnesota, USA	< 4.95	Streets, 2008
2007	Minnesota, USA	< 5.04	Streets, 2008
2007	Minnesota, USA	40.90	Streets, 2008
2007	Minnesota, USA	60.30	Streets, 2008
2007	Minnesota, USA	< 5.08	Streets, 2008
2007	Minnesota, USA	< 5.15	Streets, 2008
2007	Minnesota, USA	489.00	Streets, 2008
2007	Minnesota, USA	80.20	Streets, 2008
2007	Minnesota, USA	18.30	Streets, 2008
2007	Minnesota, USA	32.90	Streets, 2008
2007	Minnesota, USA	< 5.14	Streets, 2008
2007	Minnesota, USA	15.80	Streets, 2008
2007	Minnesota, USA	< 5.19	Streets, 2008
2007	Minnesota, USA	< 5.03	Streets, 2008

<b>Sampling Year</b>	<b>Sampling Location</b>	<b>PFOS in effluent (ng L<sup>-1</sup>)</b>	<b>Reference</b>
2007	Minnesota, USA	7.84	<i>Erickson et al., 2009</i>
2007	Minnesota, USA	545.00	<i>Erickson et al., 2009</i>
2007	Minnesota, USA	< 5.15	<i>Erickson et al., 2009</i>
2007	Minnesota, USA	< 4.97	<i>Erickson et al., 2009</i>
2007	Minnesota, USA	< 9.87	<i>Erickson et al., 2009</i>
2007	Minnesota, USA	20.50	<i>Erickson et al., 2009</i>
2007	Minnesota, USA	11.00	<i>Erickson et al., 2009</i>
2007	Minnesota, USA	91.50	<i>Erickson et al., 2009</i>
2007	Minnesota, USA	5.24	<i>Erickson et al., 2009</i>
2007	Minnesota, USA	6.00	<i>Erickson et al., 2009</i>
2007	Minnesota, USA	16.40	<i>Erickson et al., 2009</i>
2007	Minnesota, USA	15.20	<i>Erickson et al., 2009</i>
2007	Minnesota, USA	< 4.99	<i>Erickson et al., 2009</i>
2008	Washington, USA	8.53	<i>Furl et al., 2011</i>
2008	Washington, USA	31.20	<i>Furl et al., 2011</i>
2008	Washington, USA	4.42	<i>Furl et al., 2011</i>
2008	Washington, USA	3.86	<i>Furl et al., 2011</i>
2008	Washington, USA	11.70	<i>Furl et al., 2011</i>
2008	Washington, USA	18.10	<i>Furl et al., 2011</i>
2008	Washington, USA	9.36	<i>Furl et al., 2011</i>
2008	Washington, USA	10.20	<i>Furl et al., 2011</i>

a) Canada

<b>Sampling Year</b>	<b>Sampling Location</b>	<b>PFOS in effluent (ng L<sup>-1</sup>)</b>	<b>Reference</b>
2004	Ontario, Canada	42.50	<i>Furdui et al., 2008</i>
2004	Ontario, Canada	67.00	<i>Furdui et al., 2008</i>
2004	Ontario, Canada	208.50	<i>Furdui et al., 2008</i>
2004	Ontario, Canada	9.70	<i>Furdui et al., 2008</i>
2004	Ontario, Canada	8.60	<i>Furdui et al., 2008</i>
2004	Ontario, Canada	72.00	<i>D'eon et al., 2009</i>
2004	Ontario, Canada	9.90	<i>D'eon et al., 2009</i>
2004	Ontario, Canada	1.80	<i>D'eon et al., 2009</i>
2004	Ontario, Canada	6.10	<i>D'eon et al., 2009</i>
2004	Ontario, Canada	2.60	<i>D'eon et al., 2009</i>
2007	Ontario, Canada	<0.08	<i>D'eon et al., 2009</i>
2007	Ontario, Canada	0.08	<i>D'eon et al., 2009</i>
2009-2010	Canada	2.85	<i>Guerra et al., 2014</i>
2009-2010	Canada	3.94	<i>Guerra et al., 2014</i>
2009-2010	Canada	5.07	<i>Guerra et al., 2014</i>
2009-2010	Canada	3.4	<i>Guerra et al., 2014</i>
2009-2010	Canada	<2.05	<i>Guerra et al., 2014</i>
2009-2010	Canada	3.45	<i>Guerra et al., 2014</i>
2009-2010	Canada	2.55	<i>Guerra et al., 2014</i>

<b>Sampling Year</b>	<b>Sampling Location</b>	<b>PFOS in effluent (ng L<sup>-1</sup>)</b>	<b>Reference</b>
2009-2010	Canada	6.64	<i>Guerra et al., 2014</i>
2009-2010	Canada	4.7	<i>Guerra et al., 2014</i>
2009-2010	Canada	4.67	<i>Guerra et al., 2014</i>
2009-2010	Canada	25.3	<i>Guerra et al., 2014</i>
2009-2010	Canada	9.96	<i>Guerra et al., 2014</i>
2009-2010	Canada	6.1	<i>Guerra et al., 2014</i>
2009-2010	Canada	7.23	<i>Guerra et al., 2014</i>
2009-2010	Canada	2.53	<i>Guerra et al., 2014</i>
2009-2010	Canada	5.26	<i>Guerra et al., 2014</i>
2009-2010	Canada	<2.01	<i>Guerra et al., 2014</i>
2009-2010	Canada	<2.01	<i>Guerra et al., 2014</i>
2009-2010	Canada	7.39	<i>Guerra et al., 2014</i>
2009-2010	Canada	<2.06	<i>Guerra et al., 2014</i>
2009-2010	Canada	<2.06	<i>Guerra et al., 2014</i>
2009-2010	Canada	5.29	<i>Guerra et al., 2014</i>
2009-2010	Canada	3.57	<i>Guerra et al., 2014</i>
2009-2010	Canada	6.05	<i>Guerra et al., 2014</i>
2009-2010	Canada	5.23	<i>Guerra et al., 2014</i>
2009-2010	Canada	<2.05	<i>Guerra et al., 2014</i>
2009-2010	Canada	61.8	<i>Guerra et al., 2014</i>
2009-2010	Canada	294	<i>Guerra et al., 2014</i>
2009-2010	Canada	5.62	<i>Guerra et al., 2014</i>
2009-2010	Canada	18	<i>Guerra et al., 2014</i>
2009-2010	Canada	4.27	<i>Guerra et al., 2014</i>
2009-2010	Canada	2.99	<i>Guerra et al., 2014</i>
2009-2010	Canada	3.11	<i>Guerra et al., 2014</i>
2009-2010	Canada	7.81	<i>Guerra et al., 2014</i>
2009-2010	Canada	818	<i>Guerra et al., 2014</i>
2009-2010	Canada	1237	<i>Guerra et al., 2014</i>
2009-2010	Canada	9.36	<i>Guerra et al., 2014</i>
2009-2010	Canada	6.15	<i>Guerra et al., 2014</i>
2009-2010	Canada	18.3	<i>Guerra et al., 2014</i>
2009-2010	Canada	17.7	<i>Guerra et al., 2014</i>

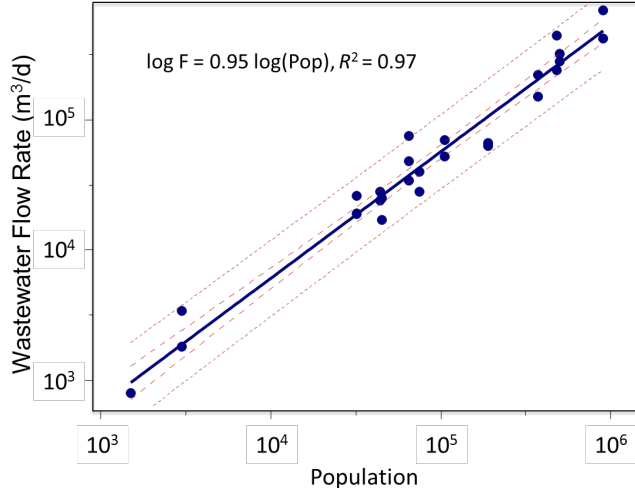


**Figure S2.** Relationship between wastewater flow rates ( $\text{m}^3 \text{ d}^{-1}$ ) and population in Canada and the U.S. Flow rates and populations served by wastewater treatment plants were available for 16 out 19 locations in Canada [Guerra *et al.*, 2014] and all U.S. locations [U.S., EPA, 2008]. Wastewater information for Canada is based on the 2009 Municipal Water and Wastewater Survey (MWWS) [*Environment Canada*, 2009]. Information on wastewater treatment facilities in the USA from the Clean Watersheds Needs Survey (CWNS) 2008 Report to Congress. We estimated the populations served for the three Canadian WWTPs lacking populations served by extrapolating the relationship shown above.

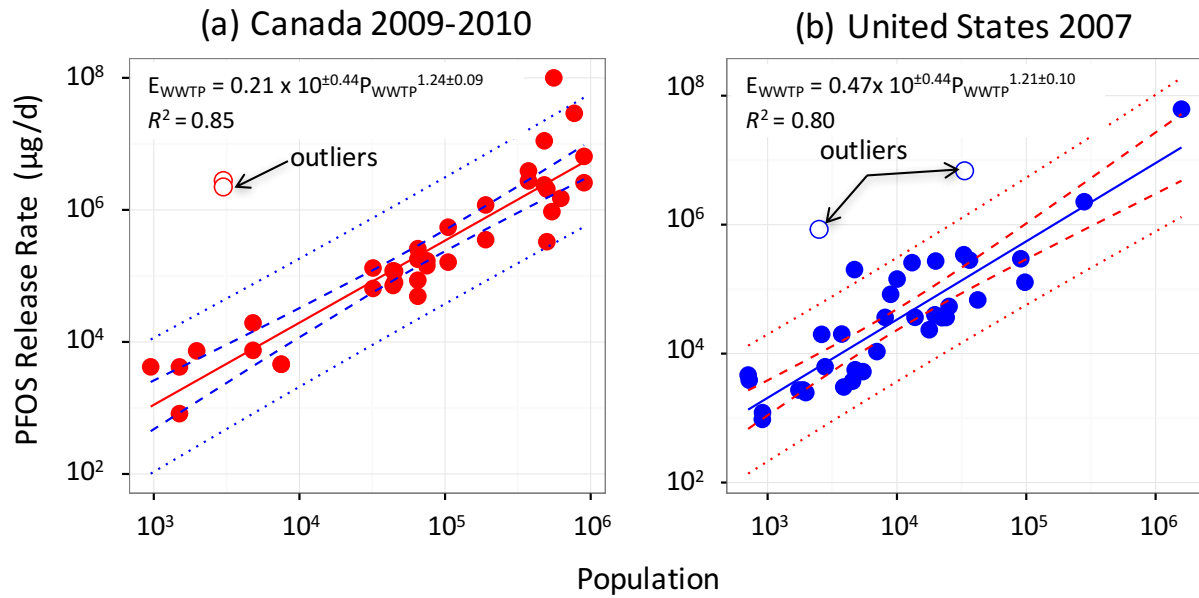


**Figure S3.** Relationships between population served by wastewater treatment plants (WWTPs) and PFOS discharges for: (a) Canadian wastewater [Guerra *et al.*, 2014], and (b) U.S. wastewater [Erikson *et al.*, 2009]. Solid lines show means derived from linear regression, dashed lines denote 95% confidence intervals around the mean, and outer dotted lines indicate the 95% confidence intervals for predictions. For data from Canada (panel a), two outliers were excluded from the regression based on results of a Bonferroni test [Weisberg, 2013] ( $p = 0.016$  and  $0.031$ ). These samples were from a wastewater treatment facility where 80% of the influent was contributed by industry [Guerra *et al.*, 2004]. Similarly, two outliers (Bonferroni outlier test:  $p = 0.020$  and  $0.046$ ) were identified for the U.S. data (panel b).

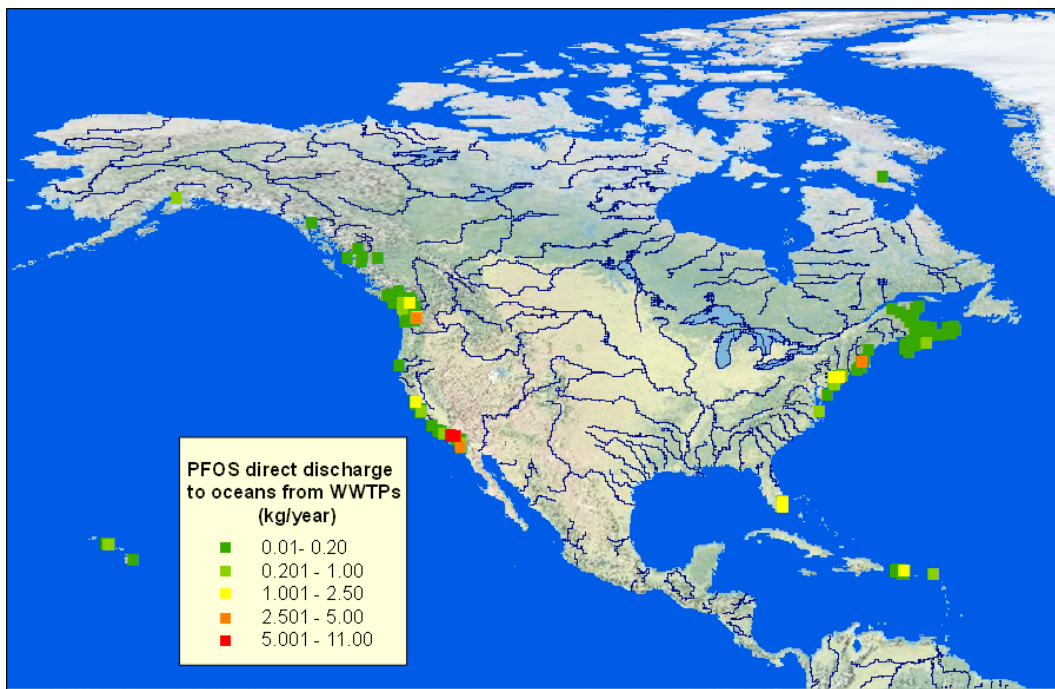


**Figure S4.** Direct PFOS discharges in wastewater to North America estuaries ca. 2010.

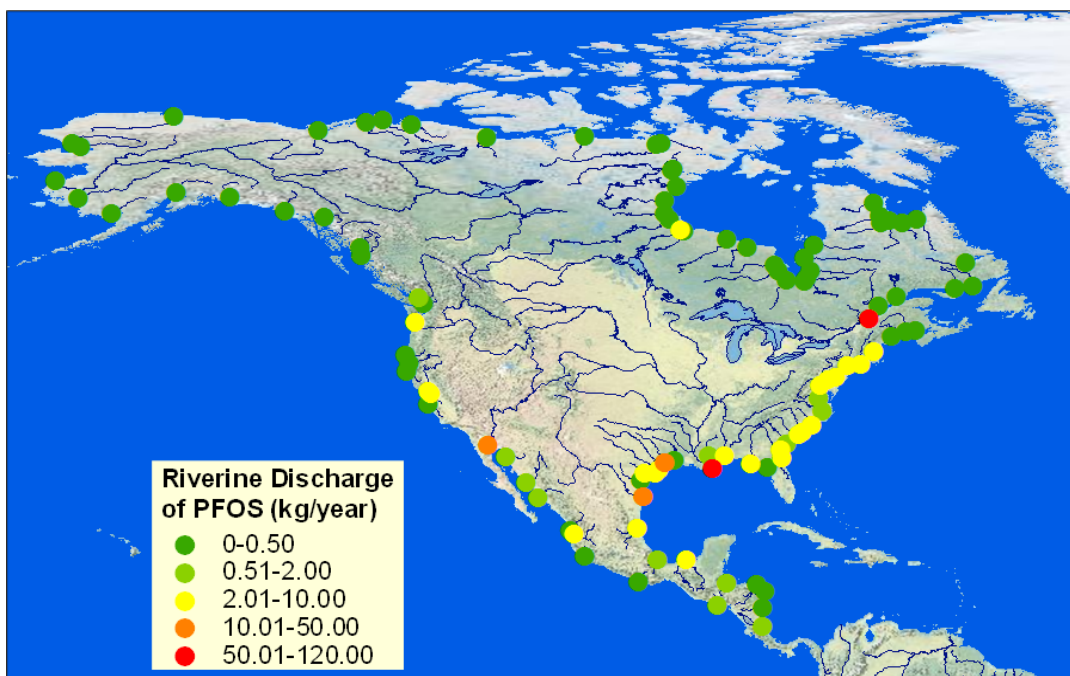


**Figure S5.** PFOS discharges ( $\text{kg a}^{-1}$ ) in 2010 from rivers in North America to the ocean.

**Table S2.** Direct PFOS discharges to estuaries ( $\text{kg a}^{-1}$ ) from wastewater treatment plants ( $> 1 \text{ kg a}^{-1}$ ) in Canada and the U.S. ca. 2010.

State/ Province, Country	City	Wastewater Treatment Plant Service Population	Latitude	Longitude	Estimated PFOS Discharge ( $\text{kg a}^{-1}$ )
CA, USA	Playa Del Rey	3780562	33.9	-118.4	11.0
CA, USA	Carson	2390090	33.8	-118.3	6.2
CA, USA	Huntington Beach	2217100	33.7	-117.9	5.7
CA, USA	San Diego	1855700	32.7	-117.2	4.5
MA, USA	Boston	1693288	42.4	-71.0	4.1
WA, USA	Seattle	1692873	47.4	-122.3	4.1
CA, USA	Huntington Beach	1293904	33.7	-117.9	2.9
FL, USA	Miami	1101000	25.7	-80.2	2.4
WA, USA	Renton	1073138	47.5	-122.2	2.3
FL, USA	Miami	946000	25.9	-80.1	2.0
NJ, USA	Sayreville	790361	40.5	-74.3	1.6
PR, USA	San Juan	767297	18.4	-66.2	1.5
BC, Canada	Vancouver	639489	49	-123	1.2
CA, USA	San Francisco	604625	37.7	-122.4	1.1
FL, USA	Pompano Beach	560715	26.3	-80.2	1.0
NY, USA	Wantagh	550000	40.7	-73.5	1.0

**Table S3.** Estimated 2009-2010 PFOS discharges > 2 kg a<sup>-1</sup> from watersheds to the oceans.

River, Country	PFOS discharge (kg a <sup>-1</sup> )	River, Country	PFOS discharge (kg a <sup>-1</sup> )
Mississippi River, USA	92	Alabama & Tombigbee Rivers, USA	4
St. Lawrence River, Canada	82	Apalachicola River, Florida	4
Colorado River (Pacific Ocean), USA	17	Santee River, USA	4
Rio Bravo (Rio Grande), USA	14	Susquehanna River, USA	4
Trinity River (Texas), USA	11	St. Johns River, Canada	4
Delaware River, USA	10	San Antonio River, USA	3
Columbia River, USA	9	Colorado River (Caribbean Sea), USA/Mexico	3
Nelson River, Canada	9	Brazos River, USA	3
Potomac River, USA	8	San Joaquin River, USA	3
Panuco River, Mexico	7	Pee Dee River, USA	3
Sacramento River, USA	7	Grisalva River, Mexico	2
Rio Grande de Santiago, Mexico	5	Connecticut River, USA	2
Hudson River, Canada	5	Merrimack River, USA	2
Altamaha River, USA	5	Cape Fear River, USA	2

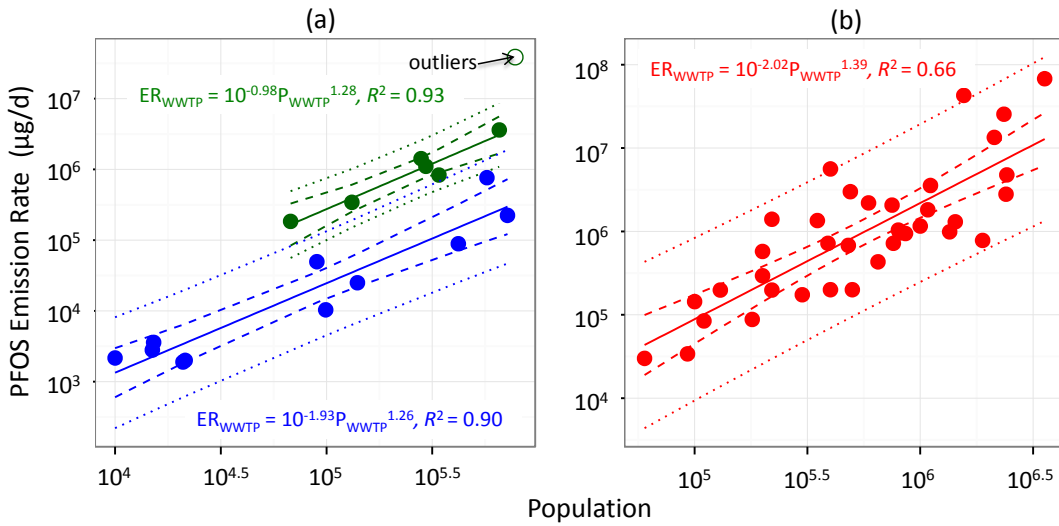


**Figure S6.** Relationships between measured PFOS and population for: (a) European wastewater sampled in 2009-2010 from 7 facilities in Northern Europe (green circles) and 11 facilities in Eastern Europe (blue points) reported in *Filipovic et al.* [2013]; (b) Chinese wastewater sampled from 37 facilities from various years summarized in *Xie et al.* [2013]. The solid line represents the best fit for observed data with 95% confidence intervals around the mean indicated by dashed lines and 95% confidence intervals around predictions indicated by the dotted line. Information on effluent flow rates and populations served from the U.S. EPA Clean Watersheds Needs Survey (CWNS) database [*U.S. EPA*, 2008].

**Table S4.** Estimated time-lags in PFOS inputs to the ocean from rivers with flows mediated by large water bodies.

System	Observed PFOS in water <sup>a</sup>	Outflow ( $10^6$ $\text{m}^3 \text{ a}^{-1}$ )	Mixing volume ( $\text{m}^3$ ) <sup>b</sup>	Estimated Lag (years)
	( $\text{ng L}^{-1}$ )/year			
St. Lawrence R., Canada (Lake Ontario)	7.0 / 2005	400	750	2.3
Nelson R., Canada (Lake Winnepeg)	0.6 / 2008	136	285	1.9
Danish Straits, Denmark (Baltic Sea)	0.2 / 2007	950	1750	3.3

<sup>a</sup> Measured PFOS data are from *Scott et al. [2009]* and *Kirchgeorg et al. [2010]*.

<sup>b</sup> Well-mixed volumes of water for each inland water body (Lake Ontario, Lake Winnepeg, Baltic Sea) are estimated from observed PFOS concentrations for a given year, cumulative inputs from this work, and losses estimated from the volume of outflowing water. Mixing volumes are then used to predict the resulting time lag of inputs and outflows.

## **Section 2: Supplemental modeling results**

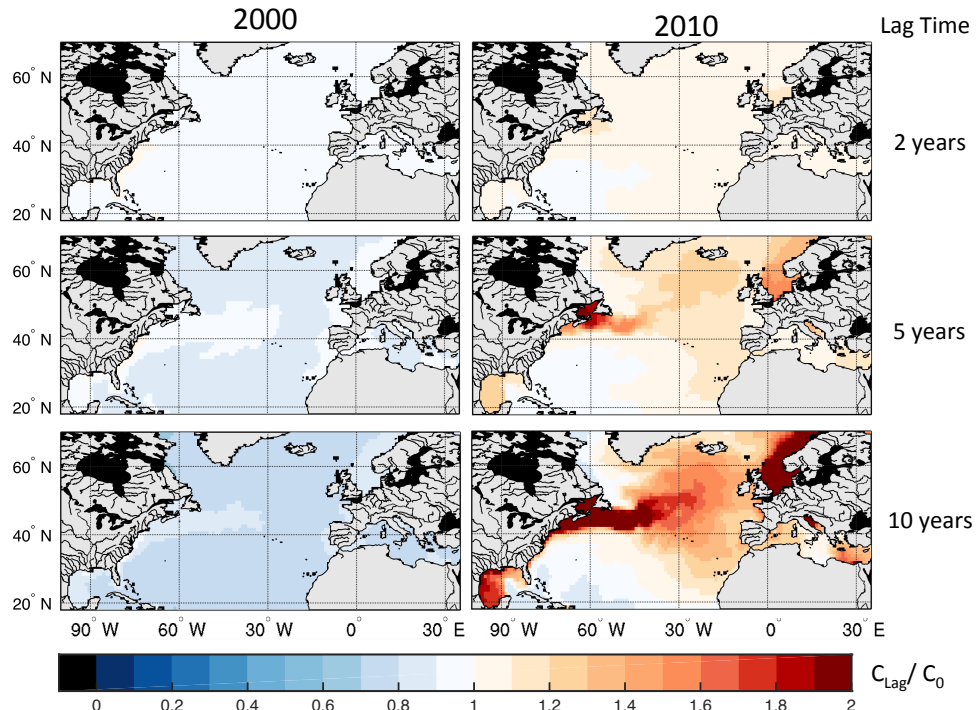


**Figure S7.** Sensitivity analysis on the effect of PFOS retention over the continent on modeled concentration in surface seawater in 2000 (peak release year) and 2010.  $C_{\text{Lag}}/C_0$  represents the difference between simulation with new lag time and the base simulation that assumes all releases reach the ocean within one year, except for rivers with large mediating water bodies (Table S4).

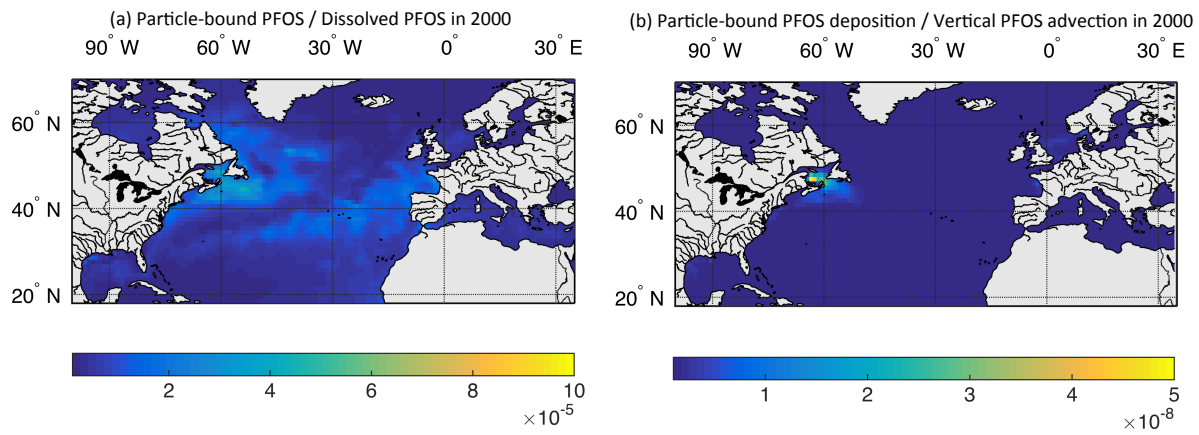


**Figure S8.** Comparison of concentrations and transport of particle-bound and dissolved PFOS.

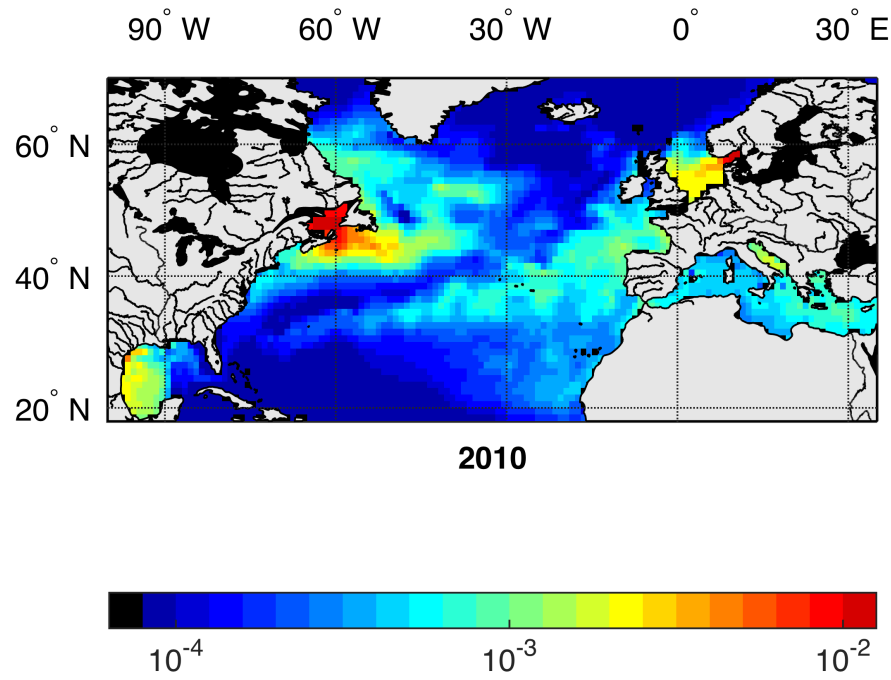


**Figure S9.** Modeled concentrations of particle-bound PFOS (pg/L) in 2010 in the North Atlantic Ocean.

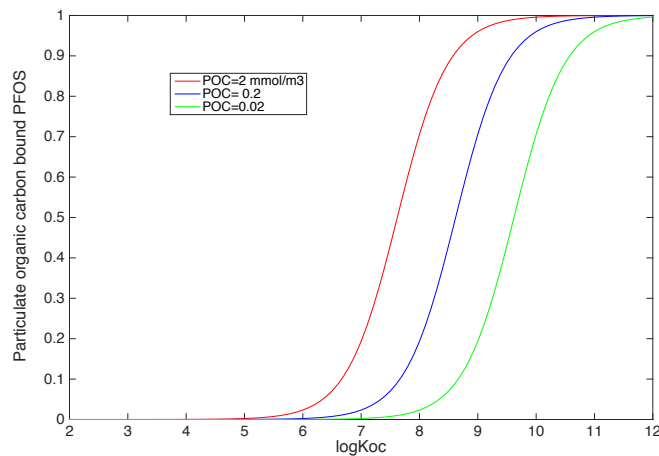


**Figure S10.** Influence of organic carbon normalized particle/water distribution coefficient ( $K_{oc}$ ) on particle-bound fraction of PFOS under difference assumptions regarding particulate organic carbon (POC) concentrations. Observed ranges of  $\log K_{oc}$  for PFOS reach a maximum of approximately 4 in the literature, suggesting the particulate fraction is generally a low proportion of the overall total PFOS reservoir.